铝合金变极性等离子焊接电弧产热机理

韩永全[1]，　陈树君[2]，　殷树言[2]
（1. 内蒙古工业大学 材料学院，呼和浩特　010051；
2. 北京工业大学 机械与应用电子技术学院，北京　100022）

韩永全

摘　要：从铝合金变极性等离子焊接电弧物理特性出发，研究了铝合金变极性等离子焊接电弧产热机理，分析了焊接参数对电弧热的影响规律。通过理论分析和试验研究，发现铝合金变极性等离子弧焊接时不对称电极特性对正、反极性期间电弧的产热具有很大的影响。反极性期间由于铝合金作为阴极，阴极压降大电弧产热量也增大。在变极性等离子弧焊接时正、反极性期间的焊接电流和持续时间等参数不同也是造成正、反极性等离子电弧产热不同的重要原因。

关键词：变极性等离子电弧；电特性；铝合金
中图分类号：TG439.5　　文献标识码：A　　文章编号：0253－360X(2007)12－035－04

0　序　　言

铝及其合金由于重量轻、比强度大和耐腐蚀性能好，在航空航天领域得到广泛的应用。但因铝合金导热快、易变形和焊缝中容易产生气孔等原因，对焊接方法及工艺要求较严格。变极性等离子弧(VPPA)焊接方法与其它熔化焊接方法相比，具有能量集中、电弧挺度大、一次穿透深度大、焊后变形小等特点[1,2]。铝合金变极性穿孔等离子弧焊接工艺在航空航天重要结构的焊接中具有良好的应用前景，并且欧美发达国家早已应用到实际生产中。国内虽然有不少学者对该工艺进行研究[3]，但由于该工艺影响因素多、对设备精度及可靠性要求高，因此对铝合金变极性等离子电弧产热机理方面研究的人极少。作者自行研制开发了微机控制的双逆变 VPPA －2 型铝合金变极性等离子弧焊接电源，并建立了基于工控机的焊接过程信号检测及分析系统，定量分析了焊接参数对变极性等离子电弧产热的影响。这对合理选择变极性等离子弧焊接参数，实现穿孔熔池热平衡具有重要的理论和实际意义。

1　试　　验

试验采用自行研制的变极性等离子弧焊接电源。焊接主电源是以 80C196KC 单片机为控制核心，主电路为双逆变型电路拓扑结构。电源正、反极性最大输出电流可达 400 A，正极性时间的调节范围为 1～999 ms，反极性时间的调节范围为 1～99 ms。微机还通过对离子气流量控制器和步进电机驱动器的控制，对离子气流量和焊接速度进行精确控制。基于工控机的焊接过程信号检测及分析系统，对焊接过程电流、电压信号进行实时检测，并且能够分别对变极性等离子电弧正、反极性电压进行分析。试验材料为 LD10 铝合金。

2　变极性等离子电弧产热机理

2.1　正极性等离子电弧的产热

焊接电弧的产热是将电能转化为热能的结果。电弧特性不同产热机理也有所不同。焊接过程中母材金属的受热是通过电弧辐射和对流进行的。在加热斑点上的比热流分布，可以近似地用高斯分布来描述。电弧中心任意点的比热流可表示为[4]

$$q(r)=q_{\mathrm{m}}\mathrm{e}^{-Kr^2}, \tag{1}$$

式中：$q(r)$为任意点的比热流；q_{m} 为加热中心斑点的最大比热流；K 为能量集中系数；r 为距测试点的距离。加热母材的电弧热功率 q 为

$$q=\int_F q(r)\mathrm{d}F=\int_0^{\infty} q_{\mathrm{m}}\mathrm{e}^{-Kr^2}2\pi r\mathrm{d}r, \tag{2}$$

$$q=\frac{\pi}{K}q_{\mathrm{m}},$$

收稿日期：2007－03－20
基金项目：国家自然科学基金资助项目(50764007)；内蒙古自治区高校科研项目(NJ06066)

$$q=\eta IU,$$

式中：η, I, U, F 分别为电弧热效率、焊接电流、电弧电压和立体高斯曲线。

变极性穿孔等离子电弧与自由电弧和直流等离子电弧等相比具有独特的特性，如正、反极性期间焊接参数、电特性不同，等离子电弧形态也不同，从而使焊接电弧的产热机理与上述电弧有所不同。

图 1 为基于工控机的焊接过程信号检测及分析系统采集到的 15 mm 厚 LD10 铝合金焊接电流及电压波形[5]。

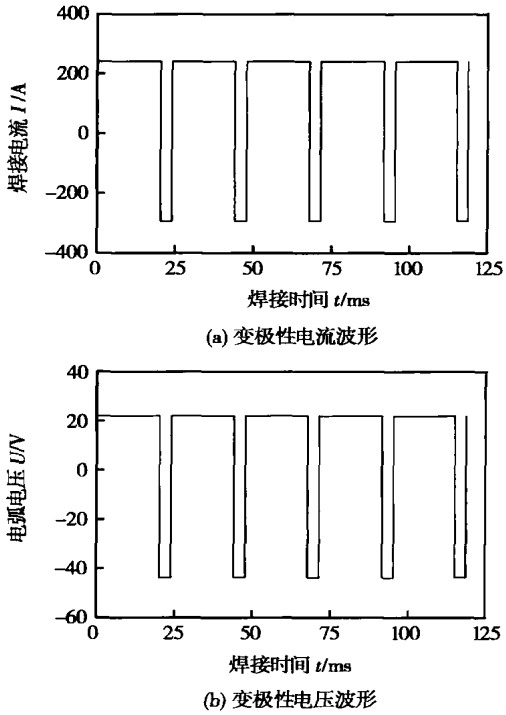

图 1 变极性等离子弧焊接电流和电弧电压波形

Fig. 1 Current and voltage of VPPA

如果按照电弧的温度为 20 000 K，根据弧柱的温度等效电压公式，计算出弧柱的等效电压为

$$U_T=\frac{2kT}{e},\qquad(3)$$

式中：k 为玻尔兹曼常数；T 为电弧温度。大电流焊接时金属电极阳极压降不超过 1 V，此时铝合金工件作为阳极的产热为

$$P_A=(U_A+U_W+U_T)\cdot I,\qquad(4)$$

式中：P_A 为阳极区产热；U_A 为铝合金作为阳极时的阳极压降；U_W 为 Al_2O_3 的逸出功；U_T 为弧柱的温度等效电压。根据图 1 实际焊接电流、电压值分别为 240 A，24 V 得正极性期间等离子电弧功率为

$$P_A=IU,\qquad(5)$$

式中：U 为正极性电弧电压（U_A, U_W, U_T 之和）；I 为焊接电流。

在自由电弧（如 TIG 焊）状态下焊接电流为 240 A 时，电弧功率约 4.50 kW，因此式(5)计算结果充分反映了等离子电弧由于压缩而电弧功率密度增多的现象。

2.2 反极性等离子电弧的产热

在交流 TIG 焊中，正极性时工件作为阳极，接受从阴极发射过来的电子释放出的逸出功，产生大量的热。因而正极性期间钨极作为阴极时，传递到工件的热量要大于反极性期间钨极作为阳极时传递到工件的热量。然而研究发现，在铝合金变极性等离子弧焊接工艺中，输入到铝合金工件上的热量并不随反极性时间在整个焊接周期中所占比例的增大而减小。虽然在很大的范围内调节反极性时间的比例，但是电弧的效率几乎是维持不变的。反极性期间，电弧效率基本维持不变的根本原因在于，与钨极相比，铝合金作为冷阴极时的阴极压降远大于钨极作为阴极时的压降。此时等离子电弧空间电子主要依靠电场来发射电子。从图 1 看出正极性电弧电压为 24 V，而反极性电弧电压为 44 V。场致发射与热发射的根本区别在于场致发射电子是依靠电极表面的强电场使电极中的电子从电极表面发射出来，并不消耗电极的逸出功，因而不会对电极产生冷却作用，可以在电极表面产生大量的热。

变极性穿孔等离子弧焊接工艺中，电弧的热效率并不随反极性时间在一个焊接周期中所占比例的改变而改变。从图 1 焊接电流和电弧电压的波形可看到反极性期间的焊接电流为 300 A，与正极性的焊接电流 240 A 相比增大 60 A，反极性时的电弧电压为44 V，几乎为正极性期间电弧电压 24 V 的 2 倍。因此在变极性等离子弧焊接过程中正常焊接参数条件下，反极性等离子电弧的产热量远远大于正极性等离子电弧的产热量。根据阴极产热公式

$$P_K=(U_K-U_W-U_T)\cdot I,\qquad(6)$$

式中：P_K 为阴极区产热；U_K 为铝的阴极压降；U_W 为 Al_2O_3 的逸出功。

从式(5)或式(6)的计算结果得知，在铝合金变极性等离子弧焊接过程正极性时输出的功率仅为反极性时输出功率的 44%，由于电弧的热效率不受反极性时间的影响，因而反极性期间单位时间内输入到工件的能量约为正极性期间的 2 倍。这一结果充

分说明了变极性等离子电弧的热特性，为铝合金变极性等离子弧焊接参数选择提供了理论支持。

3　理论分析

变极性穿孔等离子弧焊接电弧在正、反极性期间产热量的不同，反映了正、反极性等离子弧电特性的不同。图 2 为基于工控机的焊接过程信号检测及分析系统采集到的电流、电压波形，反映了随焊接电流的变化正、反极性等离子电弧电压的变化。图 2a 为正、反极性焊接电流分别从 40 A 增大到 250 A 时的采集波形图。图 2b 为焊接过程中的正、反极性等离子电弧电压波形图。图 2b 中上方线为反极性电压波形，下方线为正极性电压波形。

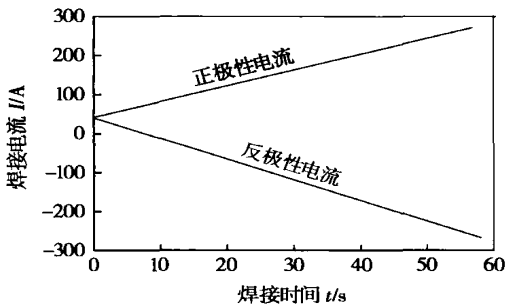

(a) 正、反极性电流波形

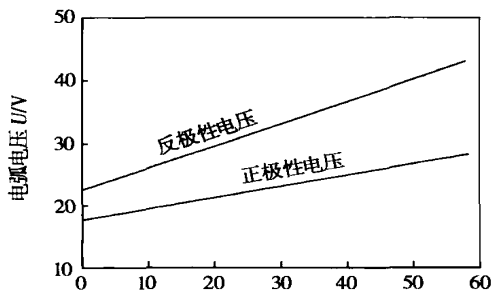

(b) 正、反极性电压波形

图 2　变极性等离子弧焊接电流和电弧电压波形

Fig. 2　Current and voltage of VPPA

图 2 说明了两个问题，一是等离子电弧电压从数值上高于自由电弧电压；二是变极性等离子电弧中反极性电弧电压高于正极性电弧电压。

图 3 为根据工控机采集到的数据而得到的变极性等离子弧特性曲线。图 3 不仅反映了变极性等离子电弧电压随焊接电流变化的规律，也反映了不同离子气流量条件下，变极性等离子电弧电压的变化规律。从 VPPA 电特性曲线上看，反极性电弧电压均比正极性电弧电压高出 10 V 左右，而且当离子气流量增大时，由于等离子电弧压缩程度的提高，电弧电压也随之提高，这是铝合金变极性等离子电弧的重要特性之一。

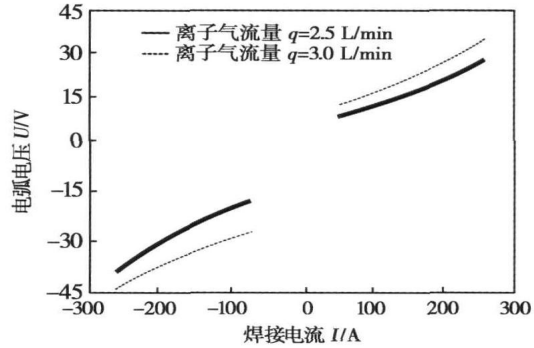

图 3　变极性等离子弧 $U-I$ 曲线

Fig. 3　$U-I$ curve of VPPA

从铝合金变极性等离子弧电特性分析可知，焊接电流和离子气流量均对变极性等离子电弧电压产生较大影响，随焊接电流和离子气流量的增大，变极性等离子电弧电压增大。厚板铝合金焊接时需要较大的热和力，通过合理匹配焊接电流和离子气流量是实现大厚板铝合金变极性等离子弧穿孔立焊工艺的关键所在。变极性等离子弧，由于电弧极性轮换变化，而且正、反极性电极特性不同，焊接参数不对称，电弧特性受多种因素影响。当变极性频率较高时热惯性对正、反极性电弧特性产生较大影响。

当然在变极性等离子弧焊接时，正、反极性等离子电弧的产热与正、反极性焊接电流的选择有关，焊接电流大电弧电压也随之增大，等离子电弧产热量必然增大。

4　结　　论

(1) 铝合金变极性等离子电弧正、反极性期间产热不同是由于反极性期间铝合金作为冷阴极而产生较大的阴极压降，从而使电弧功率增大所致。在正常焊接参数条件下反极性期间单位时间内输入到工件上的能量约为正极性期间的 2 倍。

(2) 铝合金在变极性等离子弧焊接时，正、反极性期间的焊接电流和持续时间等参数不同也是造成正、反极性等离子电弧产热不同的重要原因。

[下转第 42 页]

的分形特征和支持向量机阵列的点焊质量检测方法具有很强的识别能力，可以同时检测出点焊熔核尺寸缺陷和飞溅缺陷的准确率达到 84.6%。表明支持向量机模型在点焊质量无损检测方面是可行的。在实际应用中可以结合其它的检测手段来提高点焊质量检测的精度。

参考文献：

[1] Merller W S, Zhang L. Recent derelopment in aluminun alloys for the automotire industry [J]. Materials Science and Engineering A, 2001, 280: 37—49.

[2] Zhang S, Peng J G, Shi H. Ultrasonic inspection of spot welding quality[J]. Journal of HarBin Institute of Technology, 2003, 35(11): 1392—1398.

[3] Vapnike V N. The nature of statistical learning [M]. New York: Springer, 1998.

[4] Vapnik V, Golowich S, Smola A. Support vector method for function approximation, regression estimation and signal processing[C] // Adv Neural Infor Proc Syst. Cambride: MIT Press, 1997: 281—287.

[5] 边肇基, 张学工. 模式识别[M]. 北京: 清华大学出版社, 2000.

[6] Po Yhonen S, Negrea M, Arkk A. Fault diagnostics of an electrical machine with multiple support vector classifiers[C] // Proceedings of 2002 IEEE International Symposium on Intelligent Control. Vancouver, 2002.

[7] Gyuon I, Weston J, Barnhill S. Gene selection for cancer classification using support vector machines[J]. Machine Learning, 2002, 46(1—3): 389—422.

[8] 何学文, 赵海鸣. 支持向量机及其在机械故障诊断中的应用[J]. 中南大学学报(自然科学版), 2005, 36(1): 98—101.

[9] Amari S, Wu S. Improving support vector machine classifiers by modifying kernel functions[J]. Neural Networks, 1999, 12(6): 783—789.

[10] Burges C J C. A tutorial on support vector machines for pattern recognition [J]. Data Mining and Knowledge Discovery, 1998, 2(2): 8—34.

[11] 张学工. 关于统计学习理论与支持向量机[J]. 自动化学报, 2000, 26(1): 32—42.

[12] Zhang Xuegong. Introduction to statistical learning theory and support vector machines[J]. Acta Automatica Sinica, 2000, 26(1): 32—42.

[13] Burges C J C. A tutorial on support vector machine for pattern recognition[J]. Data Mining and Knowledge Discovery, 1998, 2(2): 121—167.

作者简介：刘鹏飞，男，1975 年出生，博士研究生。研究方向为焊接工艺及设备、点焊检测方法。发表论文 2 篇。

Email：llppff123@yahoo.com.cn

[上接第 37 页]

参考文献：

[1] Tomsic M, Barhorst S. Keyhole plasma arc welding of aluminum with variable polarity power[J]. Welding Journal, 1984, 63(2): 25—32.

[2] Nunes, Bayless E O. Variable polarity plasma arc welding on space shuttle external tank[J]. Welding Journal, 1984, 63(4): 27—35.

[3] Wang Huijun, Zheng Bing, Wang Qilong. Image sensing of the keyhole puddle from the front side of workpice in VPPAW of aluminum alloys[J]. China Welding, 1997, 6(2): 136—146.

[4] 周振丰, 张文钺. 焊接冶金学[M]. 北京: 机械工业出版社, 1987.

[5] 韩永全, 陈树君, 殷树言, 等. 大厚度铝合金变极性等离子弧穿孔立焊技术[J]. 机械工程学报, 2006, 42(9): 144—148.

作者简介：韩永全，男，1971 年出生，博士，副教授。主要研究方向为新型焊接电源及铝合金等离子弧焊接工艺。发表论文 10 余篇。

Email：nmhyq@sina.com

ubility, distortion of lattice, the micro-strains and residual stress.

Key words: aluminum alloy plate; welding; precipitation; grain size; residual stress

Braze-welding for dissimilar metals between copper and steel by Nd: YAG laser-plused MIG hybrid welding LEI Zhen, QIN Guoliang, WANG Xuyou, LIN Shangyang (Harbin Welding Institute, China Academy of Machinery Scicnce Technology, Harbin 150080, China). p18—20, 25

Abstract: Braze-welded joint between copper and steel could be achieved by laser-arc hybrid welding. With this method, high quality joining between T2 copper alloy sheet and galvanized steel sheet was successfully done. The results indicated that a brazed joint between copper and steel was formed, while the steel sheet in the joint was not melted. The tensile test shows that the crack initiated in the heat-affected zone of copper side, and the heat-affected zone is intenerated appreciably. Analysis of fracture appearance shows that the fracture characteristic of the joint is ductile fracture. The erodent structure of the steel and the penetration of copper atom through the crystal boundary of ferrite were not found by hish resolution electron micnoscope. Copper-iron solid solution formed around the brazing interfaces and both atoms diffused with each other. In addition, the brazing interface abounded with silicon.

Key words: laser; plused metal inert-gas arc; hybrid welding; copper; braze-welding

Effects of VPTIG welding current parameters on arc shape and weld quality FANG Chenfu[1], YU Jiajun[1], CHEN Shujun[2], SONG Yonglun[2] (1. Provincial Key Laboratory of Advanced Welding Technology, Jiangsu University of Science and Technology, Zhenjiang 212003, Jiangsu, China; 2. College of Mechanical Engineering and Applied Electronics Technology, Beijing University of Technology, Beijing 100022, China). p21—25

Abstract: With high-speed video system and memory real-time oscilloscope gathering welding current and arc shape information of variable polarity TIG (VPTIG) welding, effects of five parameters including welding current frequency, DCEP (direct current electrode positive) and DCEN (direct current electrode negative) time, DCEP and DCEN current amplitude on arc shape information and quality of weld were analyzed. The experiment showed that arc shape, arc welding pieces of power and heat input can be controlled by regulating the five parameters, which not only could control penetration, both sides of weld and liquidation district width on both sides of weld, but also reduced the loss of tungsten electrode. VPTIG welding craft for aluminum alloy with plate docking and low frequency impulse modulation were adopted, and the depth of fusion of single pass welding could reach 6 mm. Meanwhile, good appearance of weld and reliable quality of welded joint could be obtained.

Key words: variable polarity tungsten inert-gas welding; welding current; arc shape; weld quality

Laser welding of high nitrogen steel 1Cr22Mn16N Ⅲ. Microstructure and mechanical properties of welding heat-affected zone ZHAO Lin[1,2], TIAN Zhiling[1], PENG Yun[1,2], XU Lianghong[1,2], LI Ran[1,2] (1. State Key Laboratory of Advanced Steel Processes and Products, Central Iron & Steel Research Institute, Beijing 100081, China; 2. Division of Structural Materials, Central Iron & Steel Research Institute, Beijing 100081, China). p26—30

Abstract: The microstructure and mechanical properties of heat-affected zone (HAZ) of high nitrogen steel (HNS) were investigated by using thermo-simulation technique. The experimental results indicate that the microstructure in the HAZ of HNS is austenite and δ-ferrite under laser welding conditions. The hardness of the coarse-grained heat-affected zone (CGHAZ) increases when the cooling rate increases, and the one of the HAZ decreases while the peak temperature decreases. The results show that the hardness of the HAZ is higher than the one of the base metal, indicating no softening of the HAZ under appropriate welding conditions. The impact toughness of CGHAZ is improved with the increase of the cooling rate, whereas two brickle zones exist in the HAZ.

Key words: high nitrogen steel; laser welding; heat-affected zone; microstructure; mechanical properties

Stiffness coordination strategy for increasing fatigue life and its application in welded structure DING Yanchuang, ZHAO Wenzhong (School of Mechanical Engineering, Dalian Jiaotong University, Dalian 116028, Liaoning, China). p31—34

Abstract: The mechanical nature of welded structure fatigue damage is the local stress concentration, and the severity of the stress concentration is depending on the change of stiffness. From the point of stiffness coordination, the causes of stress concentration are analyzed. Based on IIW (International Institute of Welding) standards, the relative fatigue life of butt joint is calculated. Results show the fatigue life increase at least 3.86 times with the smoothened weld. The fatigue life analysis of flat beam with strengthen plate shows that the plate thickness increase 1 times i.e., the local stiffness increase 1 times, the fatigue life decrease 1 times. The two examples of IIW confirm that the stiffness coordination is very important to improve fatigue life. Based on the measured dynamic stress, the fatigue life of welded frame is predicted. Result shows that the stiffness coordination can significantly increase the fatigue life. The fatigue life prediction of welded frame is certificated by the experimentation.

Key words: welded structure; stiffness coordination; fatigue life

Principle of produced heat by arc properties in VPPA of aluminum alloy HAN Yongquan[1], CHEN Shujun[2], YIN Shuyan[2] (1. College of Materials Science and Engineering, Inner Mongolia University of Technology, Huhhot 010062, China; 2. College of Mechanical Engineering and Applied Electronics Technology, Beijing University of Technology, Beijing 100022, China). p35—37, 42

Abstract: The paper studied principle of arc produced heat in VPPA and analysed how welding parameters influence arc heat from physical properties of arc on Al alloy. It is shown that dissymmetrical electrode properties have great influence on produced heat of arc in positive and negative times. When Al alloy is used to be negative electrode, negative voltage produced more heat. Different parameters of welding current and lasting times are very important factors to produce heat in positive and negative times.

Key words: variable polarity plasma welding; electrical properties; aluminum alloy

Detection method of spot welding based on fractal and support vector machine LIU Pengfei, SHAN Ping, LUO Zhen (School of Materials Science and Engineering, Tianjin University, Tianjin 300072, China). p38—42

Abstract: Because of characteristic of fractal dimension which present quantitatively describing of complexity of a sample data series and remarkable advantage of support vector machine (SVM) in small sample classification and regression, fractal dimension of signal data series is adopted as eigenvectors, and a novel detection method based on fractal and SVM is presented. Two models based on SVM are constructed. One is about flatters of spot welding and the other is about defect of nugget size. A array of SVM is consist of these two models. The array is used to detect the two defects synchronously. It is shows that this new method fits for nondestructive detection of spot welding from analysis of experiment results. This array of SVM can detect the two defects of flatters and the little nugget size better in process of spot welding.

Key words: fractal; support vectors machine; detection; spot welding; flatter

Vibration frequency characters of chip and bonding on thermosonic flip chip bonding WANG Fuliang, HAN Lei, ZHONG Jue (School of Mechanical and Electronical Engineering, Central South University, Changsha 410083, China). p43—46

Abstract: The vibration velocity of tool tip and chip on thermosonic flip chip (TSFC) bonding was monitored with a laser Doppler vibrometer, and the "stall" phenomena was observed from the virtual value curve of vibration velocity, i. e., after the TSFC bonding started a fever milliseconds, the chip velocity decreases suddenly, while the tool tip velocity still increases. Stall indicated that the bump/pad interface has formed initial bonding strength. And the frequency characters of the vibration velocity signals were also obtained. It is found that the 3rd harmonics of chip vibration velocity signal indicates the stall phenomena, i. e., when the 3rd harmonics appeared, the stall happens. Experiment results show that little bonding force is good for produce stall.

Key words: thermosonic flip chip bonding; laser Doppler vibration measurement; spectral analysis

Effects of immediate water cooling and normalization after welding on microstructure and hardness of heat affected zone of ultra-fine grain steels welded joint ZHANG Guifeng[1], MIAO Huixia[1], ZHANG Jianxun[1], PEI Yi[1], WANG Jian[2], ZHANG Yantao[3] (1. School of Material Science and Engineering, Xi' an Jiaotong University, Xi' an 710049, China; 2. Technical Center of Anshan Iron and Steel Group Corporation, Anshan 114000, Liaoning, China; 3. Shandong Electric Power Construction No. 1 Project Company, Jinan 250100, China). p47—50

Abstract: To refine the grain size of the coarse grain heat affected zone (CGHAZ) in the gas tungsten arc welded joints of ultra-fine grain (UFG) steels of 400 MPa strength, the immediate water cooling before transformation completion and normalization after welding were performed. Their effects on the microstructure and hardness of the HAZ were investigated. The results show that although the grain size of CGHAZ does not decrease for the immediate water cooling, the width of CGHAZ decreases compared with the air cooling condition. The effective grain sizes in CGHAZ are significantly refined by first time normalization treatment after welding, while the grain sizes in the fine grain heat affected zone (FGHAZ) become coarser than those before normalization. The hardness of HAZ of the joint subjected to immediate water cooling is higher than that of the joint subjected to air cooling. The whole hardness of each joint after normalization decreases much. There is a favorable hardness match between the HAZ and the original base metal after first normalization treatment only for the immediate water cooling joint. Therefore, the immediate water cooling followed by one time normalization is recommended to refine the grain size in CGHAZ and to make the hardness of HAZ close to that of original parent materials.

Key words: ultra-fine grain steels; heat affected zone; coarse grain heat affected zone; normalization; hardness

Distribution and diffusion mechanism of Sn in interface of ZA alloy soldered joints LIU Xiuzhong, LI Shitong, CHEN Libo (School of Material Science and Engineering, Shandong University, Jinan 250061, China). p51—55

Abstract: Microstructure and its characteristic of ZA soldered joints, distribution of Sn elemont and reaction product of Sn in interface of ZA alloy soldered joints are studied by optical microscope, scanning electron microscope and electron probe microanalysis, reskectively. The results show that Sn mainly diffuses by volume diffusion and forms a wide diffusion zone. Sn in interface also reacts with some elements in parent metal. New phases such as α—CuSn and $Cu_{20}Sn_6$ are formed. The diffusion and reaction of Sn will be propitious to the bonding strengths and mechanical properties of soldered joints, which can satisfy the service performance of soldered joints.

Key words: ZA alloy; soldering; interface; diffusion of Sn

ANN prediction models for tensile properties of TIG welded